

Part III: lithium metasilicate (Li_2SiO_3)—mild condition hydrothermal synthesis, characterization and optical properties

Abdolali Alemi · Shahin Khademinia ·
Murat Sertkol

Received: 30 August 2014 / Accepted: 8 February 2015 / Published online: 20 February 2015
© The Author(s) 2015. This article is published with open access at Springerlink.com

Abstract Li_2SiO_3 nanopowders were synthesized via a non-stoichiometric 2:3 (S_1), 1:3 (S_2), 1:4 (S_3) and 1:5 (S_4) Li/Si molar ratios via hydrothermal reaction for 72 h at 180 °C in an aqua solution using Li_2CO_3 and H_2SiO_3 as raw materials. The synthesized materials were characterized by powder X-ray diffraction (PXRD) technique and Fourier transform infrared spectroscopy. PXRD data showed that the crystal structure of the obtained materials is orthorhombic with the space group of $\text{Cmc}2_1$. Also, to investigate the effect of the Li/Si molar ratio on the morphology of the obtained materials, the morphologies of the synthesized materials were studied by field emission scanning electron microscopy. The technique showed that with changing the Li/Si molar ratio from S_1 to S_4 , the morphology of as-prepared samples changed from flower structures to microrod–microsphere and then to a non-homogenous layer-like structure. Ultraviolet–visible spectra showed that the nanostructure lithium silicate powders had good light absorption properties in the ultraviolet light region. It showed that with changing the Li/Si molar ratio from S_1 to S_4 , the calculated band gap was decreased. Also, cell parameter refinement showed that with changing the Li/Si molar ratio from S_1 to S_4 the cell parameters

decreased. Photoluminescence analysis of the obtained materials was studied at the excitation wavelength of 247 nm. It showed that the emission spectra of the obtained materials had a blue shift from S_1 to S_4 .

Keywords Lithium metasilicate · Hydrothermal method · Nanomaterials · PXRD · FESEM

Introduction

Lithium silicates are important phases in silicate glass ceramics [1]. They are attracted because of their applications as CO_2 captures [2–8], lithium battery cathode materials [9], fast ion conductors [10], optical waveguides [11] and tritium breeding materials [12, 13]. Different methods have been reported to synthesize Li_2SiO_3 nanomaterials including solid state, precipitation, sol–gel, extrusion–spherodisation, rotating/melting, combustion, electrochemical and via hydrothermal. However, most of the time, a mixture of Li_2SiO_3 , $\text{Li}_2\text{Si}_2\text{O}_5$, Li_4SiO_4 and SiO_2 was obtained [9, 11, 14–21, 23]. Recently, we have reported the synthesis of lithium metasilicate nanomaterials through a hydrothermal method at 180 °C in a mixture of LiNO_3 , SiO_2 and NaOH at 2:3 Li/Si molar ratio [24]. Also, in our another work, with using Li_2CO_3 , H_2SiO_3 and NaOH raw materials at 1:2 Li/Si molar ratio at 180 °C for 48 and 72 h, the main phase was $\text{Li}_2\text{Si}_2\text{O}_5$ [25]. In the present study, a hydrothermal route was explored successfully to synthesize nanostructure Li_2SiO_3 powders in an aqua solution using Li_2CO_3 and H_2SiO_3 as raw materials.

In the present study, a hydrothermal route was explored successfully to synthesize nanostructure Li_2SiO_3 powders in a mixture of Li_2CO_3 , H_2SiO_3 and NaOH at 2:3, 1:3, 1:4 and 1:5 Li/Si molar ratios. To the best of our knowledge,

A. Alemi
Department of Inorganic Chemistry, Faculty of Chemistry,
University of Tabriz, Tabriz, Iran
e-mail: alemi.aa@gmail.com

S. Khademinia (✉)
Department of Chemistry, Semnan University, Semnan, Iran
e-mail: shahinkhademinia@gmail.com

M. Sertkol
Department of Physics Engineering, Istanbul Technical
University, Maslak 34469, Turkey
e-mail: msertkol@gmail.com

there is no report on the synthesis of nanostructure Li_2SiO_3 crystallites by these raw materials and Li/Si molar ratios. The effects of Li/Si molar ratio on the final products in phase composition and particle morphology were investigated, and the band gap energy of the as-prepared Li_2SiO_3 samples was initially estimated from UV–visible spectra. Also, cell parameter refinement and photoluminescence analysis of the obtained materials were studied.

Materials and methods

All chemicals were of analytical grade, obtained from commercial sources, and used without further purification. Phase identifications were performed on a powder X-ray diffractometer D5000 (Siemens AG, Munich, Germany) using $\text{CuK}\alpha$ radiation. Also, FT-IR spectra were recorded on a Tensor 27 (Bruker Corporation, Germany). Absorption and photoluminescence spectra were recorded on a Jena Analytik Specord 40 (AnalytikJena UK, Wembley, UK) and a PerkinElmer LF-5 spectrometer (PerkinElmer, Waltham, MA, USA), respectively. The morphology of the obtained materials was examined with a field emission scanning electron microscope (Hitachi FE-SEM model S-4160). Also, cell parameter refinement was reported by celref software version 3.

Experimental

In a typical synthetic experiment, 0.300 g (4.00 m mol) of Li_2CO_3 ($M_w = 73.82 \text{ g mol}^{-1}$) and 1.06 g (8.69 m mol), 1.46 g (24.4 m mol), 1.95 g (32.0 m mol) or 2.44 g (40.6 m mol) of H_2SiO_3 ($M_w = 60.08 \text{ g mol}^{-1}$) were added to 60 mL of hot aqueous solutions of 0.3, 0.8, 1.06 or 1.4 M NaOH under magnetic stirring at 80 °C, respectively. The resultant solution was stirred further for 15 min. The resultant solution was transferred into a 100-mL Teflon lined stainless steel autoclave. The autoclave was sealed and heated at 180 °C 72 h. When the reaction was completed, it was cooled to room temperature by water immediately. The prepared powder was washed with distilled water and dried at 110 °C for 20 min under normal atmospheric conditions. Finally, it was allowed to cool slowly to room temperature to collect a white powder.

Results and discussion

Powder X-ray diffraction analysis

The crystal phases of the hydrothermally synthesized nanomaterials at 180 °C with different Li/Si molar ratios

were examined by powder X-ray diffraction technique. As shown in Fig. 1, with the Li/Si molar ratios of 2:3, 1:3, 1:4 and 1:5 in the reaction mixture, a pure highly crystalline phase of Li_2SiO_3 (space group of $\text{Cmc}2_1$ [10, 21–24]) is obtained after 72 h. Interplanar spacing (d) in the crystalline material was calculated via Bragg's equation ($n\lambda = 2d_{\text{hkl}} \sin\theta$). So, compared to nanoparticles of pure lithium silicates, with changing the Li/Si molar ratios from 2:3 to 1:5, the diffraction lines in the powder XRD patterns of the nanoparticles of lithium metasilicate shift to a higher 2θ values ($\Delta 2\theta = 18.82$ (S_4) – 18.80 (S_1) = 0.02° and $\Delta d = 4.714526 \text{ \AA}$ (S_1) – 4.70954 (S_4) = 0.005 \AA). So, according to above measurements, there is a contraction in the unit cell with changing the Li/Si molar ratio from 2:3 to 1:5. Also, the crystal sizes were calculated by Scherrer equation at the peak with the miller indices (200) $t = \frac{k\lambda}{B_{1/2} \cos \theta}$ where t is entire thickness of the crystalline sample, λ (0.154 nm) is the X-ray diffraction wavelength, k (0.9, $B_{1/2}$) is the Scherrer constant and is of the full width at half its maximum (FWHM) intensity, and θ_B is the half diffraction angle at which the peak location is. The data summarized in Table 1 are in a good agreement with the interplanar spacing in the crystalline material measured via Bragg's equation.

Morphology analysis

Figure 2 shows the FESEM images of lithium metasilicate nanomaterials (S_1) after 72 h at 180 °C. Figure 2a shows the low-magnification image of the obtained material. It shows that the morphology of the material is a flower structure. Figure 2b, c shows that the petals of the flowers

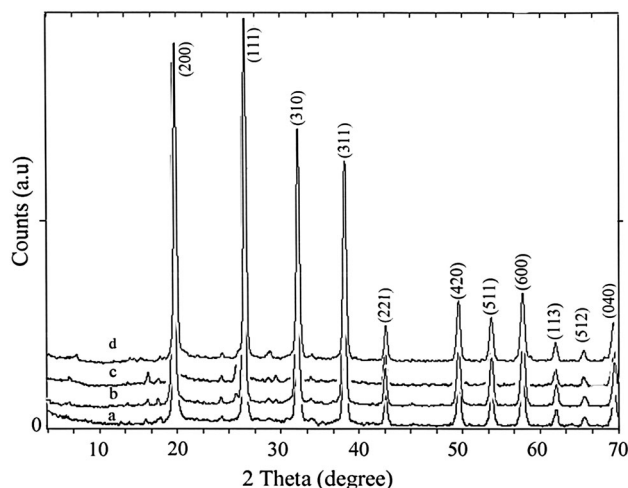
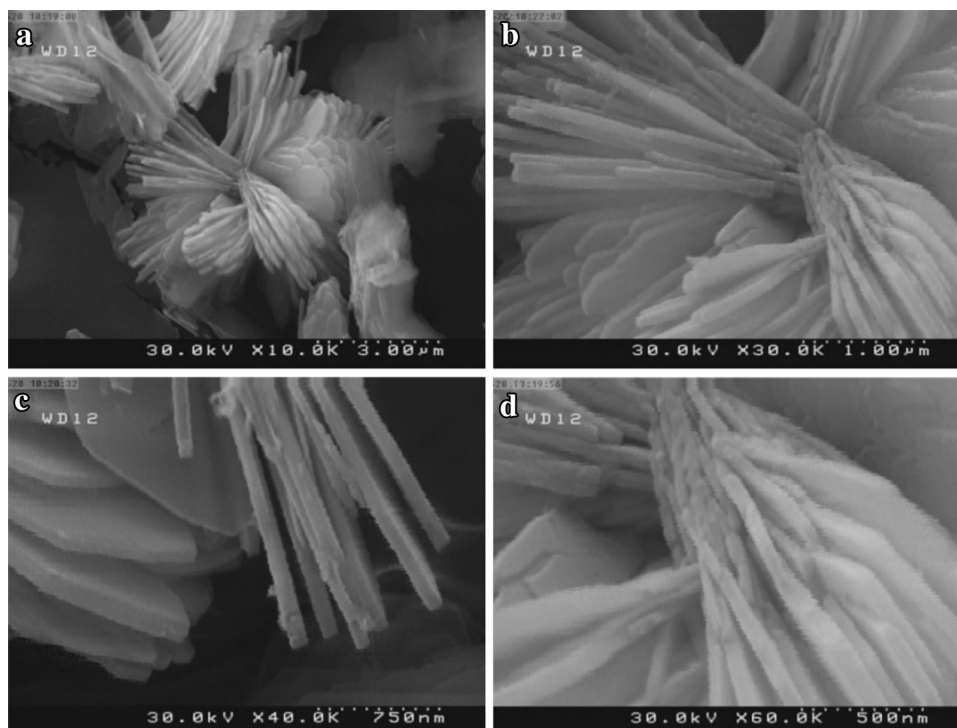


Fig. 1 PXRD patterns of the synthesized $\text{Li}_2\text{Si}_2\text{O}_5$ nanoparticles, where a (S_1) is at 2:3 Li/Si, b (S_2) is at 1:3, c (S_3) is at 1:4, and d (S_4) is at 1:5 Li/Si molar ratios



Table 1 Scherrer data information for pure Li_2SiO_3 nanomaterials obtained after 72 h at 180 °C

Data information	2θ	θ value	$B_{1/2}$ (°)	$B_{1/2}$ (radian)	$\cos\theta_b$	Crystal size (nm)
S_1	18.80	9.400	0.3193	0.00557	0.98657	25.20
S_2	18.81	9.405	0.3190	0.00556	0.98655	25.25
S_3	18.93	9.465	0.2754	0.00480	0.98639	29.25
S_4	18.82	9.410	0.3193	0.00557	0.98654	25.22

Fig. 2 SEM images of the hydrothermally synthesized Li_2SiO_3 nanomaterials obtained at 2:3 Li/Si molar ratio (S_1) after 72 h at 180 °C

have a regular edge shape joined in a point until they form a flower structure. Figure 2d shows the high-magnification image of the material. It shows that the petal thickness size is about 50 nm and the length size is about 2 μm .

Figure 3 shows the FESEM images of lithium metasilicate nanomaterials (S_2) after 72 h at 180 °C. With low magnification at Fig. 3a, b, it is clear that with changing the Li/Si molar ratio from 2:3 to 1:3, the morphology of the obtained material changed to another kind of flower-like structure. It shows that the flowers are in straw bundle-like forms to which the petals join in a certain point. With high magnification in Fig. 3c, d, it is obvious that the whole size of the flower is in about 5–7 μm , the petal thickness size is in about 60–70 nm, and the length size is in about 3 μm . Figures 2 and 3 show a general but different type of flower structure morphologies.

Figure 4 shows the FESEM images of the obtained materials (S_3) after 72 h at 180 °C. It shows that with changing the Li/Si molar ratio, the morphology changed from flower-like structure to a mixture of morphologies. Figure 4a shows the low-magnification image of the

material. It shows that the material has formed from a mixture of microrod and microspherule structures. Figure 4b, c shows that there are layer-like structures covered on the surface of the sphere particles. It shows that the sphere sizes are nearly homogenous and are about 2 μm . Also, the layer thickness sizes are about 50–70 nm (inset in Fig. 4b). Figure 4d clearly shows the rod-like structures. The thickness sizes of the rods are about 300–500 nm, and the length sizes are in about 5–8 μm .

Figure 5 shows the FESEM images of the obtained materials (S_4) after 72 h at 180 °C. It shows that with changing the Li/Si molar ratio to 1:5, the morphology changed from a mixture of sphere- and rod-like structure to a nearly layer-like structure with no certain orientation and regular shape. Figure 5c shows that the layers have no regular edge shape and the thickness sizes are about 100–120 nm. According to the data, from Figs. 2, 3, 4 and 5, by changing Li/Si molar ratio from S_1 to S_4 , it was found that the thickness of the flower petals is 50 nm for S_1 , 60–70 nm for S_2 , respectively; thickness of the rods is in about 300–500 nm for S_3 , and the thickness of the layer-

Fig. 3 SEM images of the hydrothermally synthesized Li_2SiO_3 nanomaterials obtained at 1:3 Li/Si molar ratio (S_2) after 72 h at 180 °C

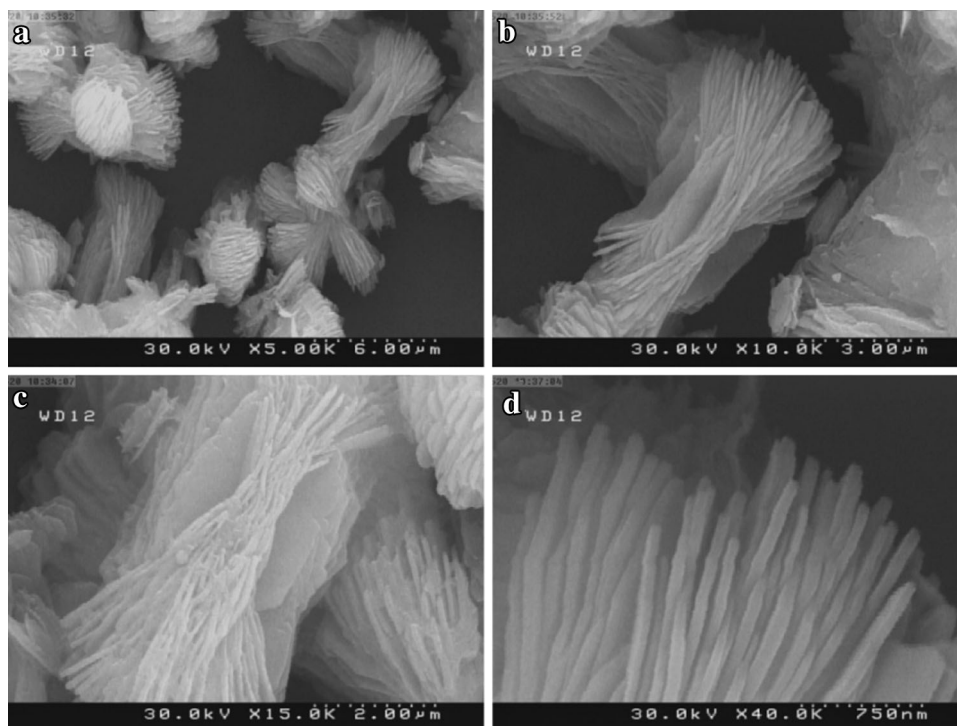
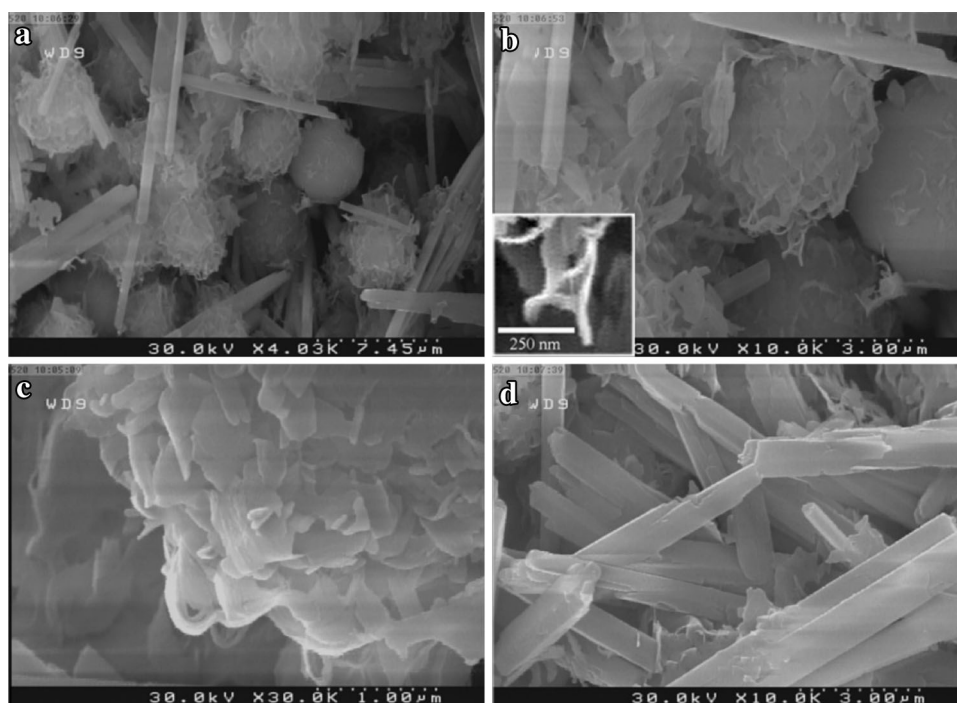


Fig. 4 SEM images of the hydrothermally synthesized Li_2SiO_3 nanomaterials obtained at 1:4 Li/Si molar ratio (S_3) after 72 h at 180 °C



like structure is about 100–120 nm. However, the crystal structure of the obtained materials is the same, and all of the obtained materials are pure phase. It shows that with decreasing the Li/Si molar ratio, the morphology of the obtained materials changed to a non-uniform structure and the thickness of the materials decreased.

Table 2 shows the cell parameter refinement data of the obtained materials at different Li/Si molar ratios. It is clear that with changing the Li/Si molar ratio from 2:3 to 1:5, parameters a, b and c decreased. However, compared to S_4 , parameter b for S_3 is larger than that for S_4 and parameters a and c are smaller than those for S_4 .

Fig. 5 SEM images of the hydrothermally synthesized Li_2SiO_3 nanomaterials obtained at 1:5 Li/Si molar ratio (S_4) after 72 h at 180 °C

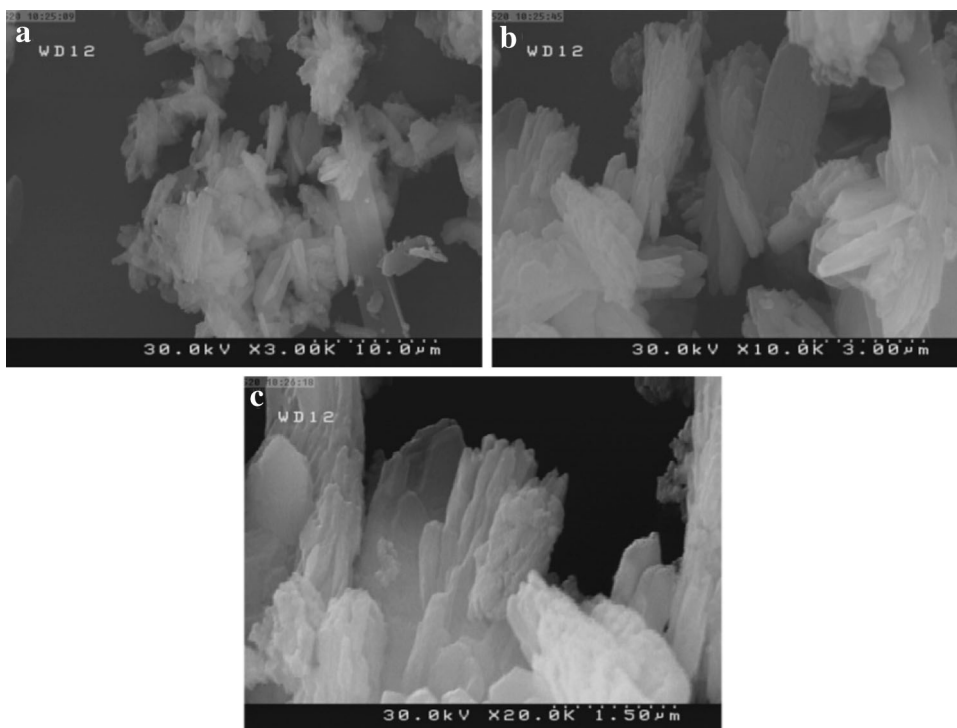


Table 2 Cell parameter refinement plot of Li_2SiO_3 showing a contraction along a and b directions in the unit cell

	a	b	c
Standard sample (pdf number 14-0322)	9.3920	5.3970	4.6600
S_1	9.3834	5.4018	4.6682
SD	0.0062	0.0032	0.0042
S_2	9.3762	5.3998	4.6678
SD	0.0076	0.0035	0.0036
S_3	9.3483	5.4039	4.6611
SD	0.0085	0.0035	0.0022
S_4	9.3767	5.3996	4.6653
SD	0.0087	0.0039	0.0048

Optical properties

Figure 6 shows the pL spectra of the obtained materials. It is clear that with changing Li/Si molar ratio from 2:3 to 1:5, the emission spectra shift to higher wavelengths. So the sharpest peaks for S_1 , S_3 and S_4 are at 542, 547 and 549 nm, respectively.

Figure 7 shows the Fourier transform infrared (FT-IR) spectra of the obtained materials S_1 and S_3 at 180 °C. The band at 416 and 520 cm^{-1} can be assigned to the bending vibration of the O–Si–O bond, and the band at 733 cm^{-1} is due to the symmetric stretching of Si–O–Si bond [26]. Besides, the peaks at 852.48 cm^{-1} are assigned to Si–O–Si

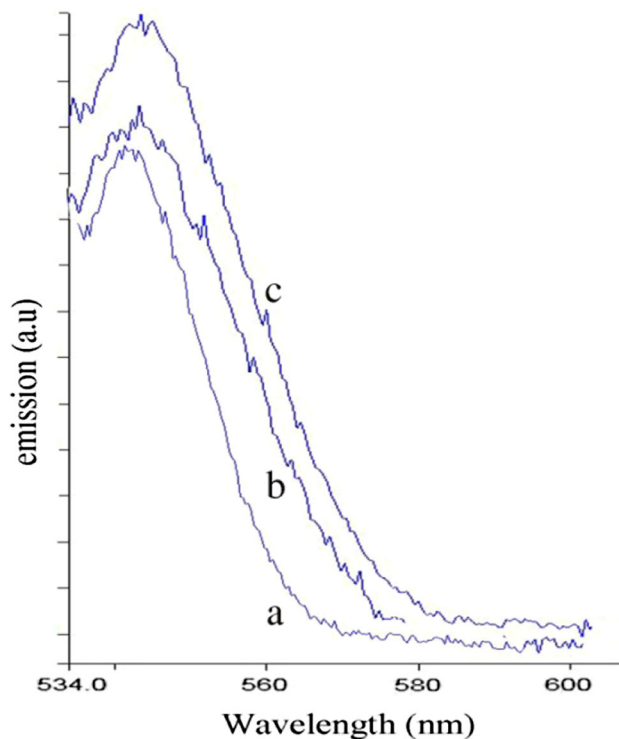


Fig. 6 Photoluminescence spectra of the synthesized Li_2SiO_3 nanomaterials ($\lambda_{\text{ex}} = 247 \text{ nm}$)

and O–Si–O stretching vibration. The band at 931 cm^{-1} is known to be caused by the non-bridging oxygen stretching mode of the Si-O^- [27, 28]. And the band at 1101 cm^{-1} is

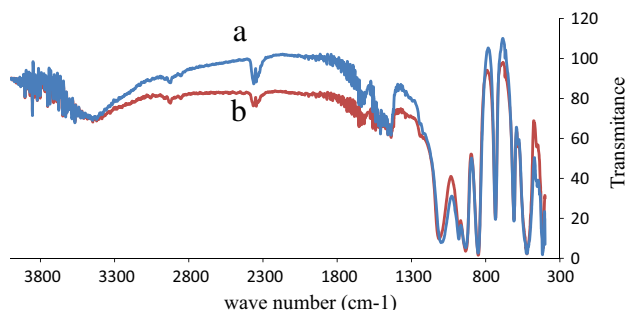


Fig. 7 FT-IR spectra of the synthesized Li_2SiO_3 nanomaterials where *a* is S_1 and *b* is S_4

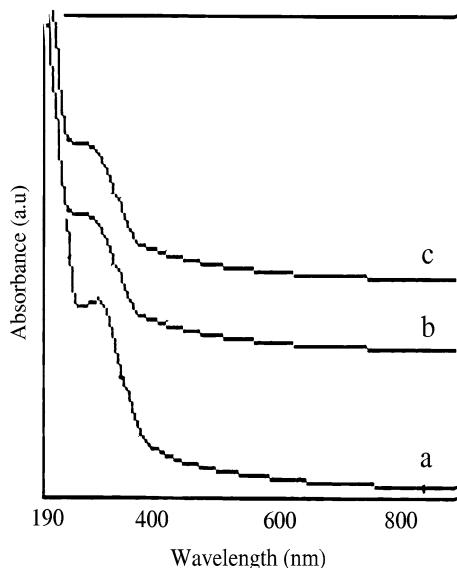


Fig. 8 UV-Vis spectra of the synthesized Li_2SiO_3 nanomaterials where *a* is S_1 , *b* is S_3 , and *c* is S_4

known to be caused by the asymmetric stretching mode of the Si–O–Si [29], and the peak at 3447.49 cm^{-1} is assigned to O–H stretching vibration [20].

Figure 8 shows the UV-Vis spectra of the obtained materials at different Li/Si molar ratios. It is clear that with changing the Li/Si molar ratio from 2:3 to 1:5, there is a red shift in the absorption wavelength. A sharp absorption band at 275, 277 and 280 nm is observed, respectively, for samples a, b and c. According to the absorption electronic spectra, the band gap of the synthesized nanomaterials is calculated to be 4.50 eV (for S_1), 4.47 eV (for S_3) and 4.425 eV (for S_4).

Conclusion

In summary, lithium metasilicate nanomaterials were successfully synthesized by a simple hydrothermal method.

We found that the Li/Si molar ratio has a major effect on the size, morphology and optical properties of the obtained products. According to the data, FESEM images showed that the morphology of as-prepared samples changed from flower structures to microrod–microsphere and then to a non-homogenous layer-like structure for S_1 to S_4 . Also, ultraviolet–visible spectra showed that the calculated band gaps decreased from S_1 to S_4 . Also, cell parameter refinement showed that with changing the Li/Si molar ratio from S_1 to S_4 , the cell parameters decreased. Photoluminescence analysis of the obtained materials at the excitation wavelength of 247 nm showed that the emission spectra of the obtained materials had a blue shift from S_1 to S_4 .

Acknowledgments The authors express their sincere thanks to the authorities of Tabriz University for financing the project.

Open Access This article is distributed under the terms of the Creative Commons Attribution License which permits any use, distribution, and reproduction in any medium, provided the original author(s) and the source are credited.

References

1. Beall, G.H.: Design and properties of glass-ceramics. *Annu. Rev. Mater. Sci.* **22**, 91–119 (1992)
2. Vincent, C.A.: Lithium batteries: a 50-year perspective, 1959–2009. *Solid State Ion.* **134**, 159–167 (2000)
3. Lu, C.H., Cheng, L.W.: Reaction mechanism and kinetics analysis of lithium nickel oxide during solid-state reaction. *J. Mater. Chem.* **10**, 1403–1419 (2000)
4. Subramanian, V., Chen, C.L., Chou, H.S., Fey, G.T.K.: Microwave-assisted solidstate synthesis of LiCoO_2 and its electrochemical properties as a cathode material for lithium batteries. *J. Mater. Chem.* **11**, 3348–3353 (2001)
5. Pfeiffer, H., Bosch, P., Bulbulian, S.: Sol–gel synthesis of $\text{Li}_2\text{ZrSi}_6\text{O}_{15}$ powders. *J. Mater. Chem.* **10**, 1255–1258 (2000)
6. Pfeiffer, H., Bosch, P.: Thermal stability and high-temperature carbon dioxide sorption on hexa-lithium zirconate ($\text{Li}_6\text{Zr}_2\text{O}_7$). *Chem. Mater.* **17**, 1704–1710 (2005)
7. Mosqueda, H.A., Vazquez, C., Bosch, P., Pfeiffer, H.: Nanoscale domain control in multiferroic BiFeO_3 thin films. *Chem. Mater.* **18**, 2307–2310 (2006)
8. Pfeiffer, H., Vazquez, C., Lara, V.H., Bosch, P.: Thermal behavior and CO_2 absorption of $\text{Li}_{2-x}\text{Na}_x\text{ZrO}_3$ solid solutions. *Chem. Mater.* **19**, 922–926 (2007)
9. Vinod, M.P., Bahnemann, D.: Materials for all-solid-state thin-film rechargeable lithium batteries by sol–gel processing. *J. Solid State Electrochem.* **7**, 493–498 (2002)
10. Zhang, B., Eastal, A.J.: Effect of HNO_3 on crystalline phase evolution in lithium silicate powders prepared by sol–gel processes. *J. Mater. Sci.* **43**, 5139–5142 (2008)
11. Cruz, D., Bulbulian, S., Lima, E., Pfeiffer, H.: Kinetic analysis of the thermal stability of lithium silicates (Li_4SiO_4 and Li_2SiO_3). *J. Solid State Chem.* **179**, 909–911 (2006)
12. Nakazawa, T., Yokoyama, K., Noda, K.: Ab initio MO study on hydrogen release from surface of lithium silicate. *J. Nucl. Mater.* **258**, 571–574 (1998)
13. Munakata, K., Yokoyama, Y.: Ab initio study of electron state in Li_4SiO_4 crystal. *J. Nucl. Sci. Technol.* **38**, 915–921 (2001)

14. Taddia, M., Modesti, P., Albertazzi, A.: Determination of macro-constituents in lithium zirconate for tritium-breeding applications. *J. Nucl. Mater.* **336**, 173–191 (2005)
15. Pfeiffer, H., Bosch, P., Bulbulian, S.: Synthesis of lithium silicates. *J. Nucl. Mater.* **257**, 309–316 (1998)
16. van der Laan, J.G., Kawamura, H., Roux, N., Yamaki, D.: Ceramic breeder research and development: progress and focus. *J. Nucl. Mater.* **283**, 99 (2000)
17. Cruz, D., Bulbulian, S.: Synthesis of Li_4SiO_4 by a modified combustion method. *J. Am. Ceram. Soc.* **88**, 1720–1724 (2005)
18. Ortiz-Landeros, J., Contreras-García, M.E., Gómez-Yáñez, C., Pfeiffer, H.: Surfactant-assisted hydrothermal crystallization of nanostructured lithium metasilicate (Li_2SiO_3) hollow spheres: (I) synthesis structural and microstructural characterization. *J. Solid State Chem.* **184**, 1304–1311 (2011)
19. Tang, T., Zhang, Z., Meng, J.B., Luo, D.L.: Synthesis and characterization of lithium silicate powders. *Fusion Eng Des.* **84**, 2124–2130 (2009)
20. Mohamed Mahmoud, M., Folz, D.C., Suchicital, T.A.C., Clark, D.E.: Crystallization of lithium disilicate glass using microwave processing. *J. Amer. Chem. Soc.* **95**, 579–585 (2012)
21. Alemi, A., Khademinia, S., Dolatyari, M., Bakhtiari, A.: Hydrothermal synthesis, characterization, and investigation of optical properties of Sb^{3+} -doped lithium silicates nanostructures. *Int. Nano Lett.* **2**, 20–29 (2012)
22. Gutierrez, G.M., Cruz, D., Pfeiffer, H., Bulbulian, S.: Low temperature synthesis of Li_2SiO_3 : effect on its morphological and textural properties. *Res. Lett. Mater. Sci.* **2**, 1 (2008)
23. Alemi, A., Khademinia, S.W., Joo, S., Dolatyari, M., Bakhtiari, A.: Lithium metasilicate and lithium disilicate nanomaterials: optical properties and density functional theory calculations. *Int. Nano Lett.* **3**, 14–25 (2013)
24. Alemi, A., Khademinia, S.: Part I: lithium metasilicate (Li_2SiO_3): mild condition hydrothermal synthesis, characterization and optical properties. *Int. Nano Lett.* **5**, 15–20 (2014)
25. Alemi, A., Khademinia, S., Sertkul M.: Lithium disilicate ($\text{Li}_2\text{Si}_2\text{O}_5$): mild condition hydrothermal synthesis, characterization and optical properties. *J. Nano Struct.* (2014, submitted)
26. El-Alaily, N.A.: Study of some properties of lithium silicate glass and glass ceramics containing blast furnace slag. *Glass Technol.* **44**, 30–35 (2003)
27. Wereszczak, A., Lara-Curzio, E., Mizuno, M.: *Advances in Bioceramics and Biocomposites II*, Ceramic Engineering and Science Proceedings. Wiley (2007)
28. Efimov, A.M.: vibrational spectra, related properties and structure of inorganic glasses. *J. Non Cryst. Solids* **253**, 95–118 (1999)
29. Efimov, A.M., et al.: Infrared reflection spectra, optical constants and band parameters of binary silicate and borate glasses obtained from water free polished sample surface. *Glass Technol.* **46**(1), 20–27 (2005)

